NANO LETTERS

pubs.acs.org/NanoLett

Fano-like Interference in Self-Assembled Plasmonic Quadrumer Clusters

Jonathan A. Fan,[†] Kui Bao,[‡] Chihhui Wu,[§] Jiming Bao,[∥] Rizia Bardhan,[⊥,▽] Naomi J. Halas,[‡,⊥] Vinothan N. Manoharan,[†,#] Gennady Shvets,[§] Peter Nordlander,[‡] and Federico Capasso*[,†]

[†]School of Engineering and Applied Sciences, Harvard University, 29 Oxford Street, Cambridge, Massachusetts 02138, United States, [‡]Department of Physics and Astronomy, Rice University, MS 61, Houston, Texas 77005, United States, [§]Department of Physics, University of Texas at Austin, 1 University Station C1600, Austin, Texas 78712, United States, [∥]Department of Electrical and Computer Engineering, University of Houston, 4800 Calhoun Road, Houston, Texas 77204, United States, [⊥]Department of Chemistry, Rice University, MS-60, Houston, Texas 77251, United States, and [#]Department of Physics, Harvard University, 17 Oxford Street, Cambridge, Massachusetts 02138, United States

ABSTRACT Assemblies of strongly interacting metallic nanoparticles are the basis for plasmonic nanostructure engineering. We demonstrate that clusters of four identical spherical particles self-assembled into a close-packed asymmetric quadrumer support strong Fano-like interference. This feature is highly sensitive to the polarization of the incident electric field due to orientation-dependent coupling between particles in the cluster. This structure demonstrates how careful design of self-assembled colloidal systems can lead to the creation of new plasmonic modes and the enabling of interference effects in plasmonic systems.

KEYWORDS Fano resonance, plasmon, coupling, self-assembly, nanoshell, nanocluster

Fano interference is a general phenomenon in systems where energy transfer from an initial state to a final state can occur via two pathways.[1] It arises when these pathways destructively interfere, reducing the total energy transfer to the final state. This effect was originally studied in atomic[1] and other quantum mechanical systems such as coupled quantum wells in semiconductors;[2] recently, classical analogues to Fano interference[3] have been studied in systems of interacting plasmonic nanostructures.[4−12]

Plasmonic systems supporting Fano-like interference can be characterized by a frequency diagram (Figure 1a) consisting of a continuum of incident photons (I), a superradiant "bright" mode (B) that couples to the continuum, and a subradiant "dark" mode (D) that does not couple to the continuum but couples to the bright mode via a near-field interaction. The bright mode is strongly lifetime broadened with a decay rate Γ_B due to radiative and nonradiative losses, such as free carrier absorption, while the dark mode is weakly lifetime broadened with a decay rate $\Gamma_D \ll \Gamma_B$ due principally to nonradiative losses. The frequency of the dark mode lies within the width of the bright mode.

If the system is pumped at frequencies resonant with both the bright and dark mode, the bright mode will be excited by two pathways (Figure 1b): $|I\rangle \rightarrow |B\rangle$ and $|I\rangle \rightarrow |B\rangle \rightarrow |D\rangle \rightarrow |B\rangle$. Coupling between $|B\rangle$ and $|D\rangle$ (Figure 1c) occurs as the near-field of one mode overlaps with and excites the other mode. Phase shifts accumulate here because the coupling occurs at the resonances of the modes and is dispersive;[3] generally, the excitation of a classical oscillator at its resonance incurs a phase shift ranging from 0 to π. Fano-like interference occurs when the cumulative phase shift from $|B\rangle \rightarrow |D\rangle \rightarrow |B\rangle$ is π so that the two pathways shown in Figure 1b interfere destructively, canceling the polarization of the bright mode. The result is a narrow window of transparency characterized by a minimum in the scattering and extinction spectrum.

Classical coupling between superradiant and subradiant modes in Fano-like interference can be modeled in several ways that highlight the underlying physical mechanism. One approach involves a mass-spring analogy, where the modes are treated as masses coupled together by a spring.[3] The "bright mass" is electrically charged and therefore couples to an external electromagnetic force and is strongly damped; the "dark mass", not being charged, does not couple to the external force and is weakly damped. By judicious choice of system parameters, the Fano minimum can be resolved in the spectrum of the bright mass amplitude. An even more general description, presented in the SOM, can be formulated by expressing the polarizability of a lossy, dipolar oscillator as the summation of a weak and strong resonance. Here, it is found analytically that near the peak of the weak resonance, the narrow Fano minimum and lineshape is recovered in the polarizability spectrum.

In many prior demonstrations of plasmonic Fano-like interference, nanostructures were fabricated with top-down

*Correspondence and requests for materials should be addressed to F.C. (capasso@seas.harvard.edu).

[▽]Current address: Molecular Foundry, Material Science Division, Lawrence Berkeley National Laboratory, Berkeley, CA 94720, United States.

Received for review: 08/23/2010
Published on Web: 10/05/2010

DOI: 10.1021/nl1029732 | *Nano Lett.* **2010,** *10,* 4680–4685

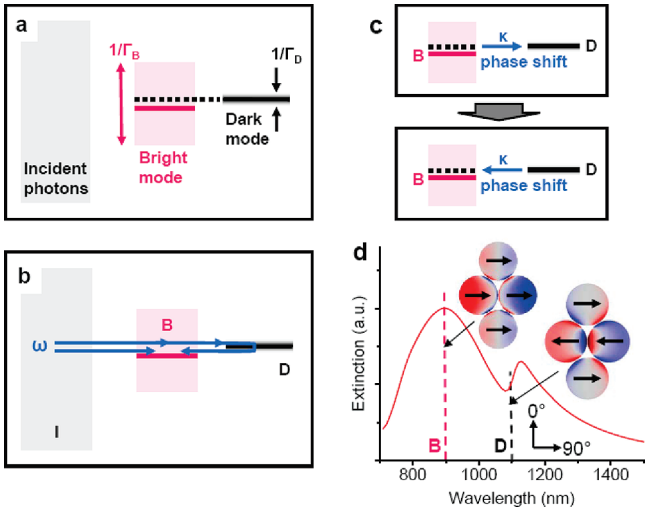

FIGURE 1. Schematics describing plasmonic Fano-like interference. (a) Frequency diagram for a system supporting Fano-like interference. There exists a bright mode, which can couple to photons in the continuum (e.g., free space), and a dark mode, which does not couple to the continuum. The modes are linewidth broadened with decay rates Γ_B and Γ_D, respectively, and they overlap in energy. (b) The excitation of the bright mode at ω can occur by two paths with degenerate energies, $|I\rangle \rightarrow |B\rangle$ and $|I\rangle \rightarrow |B\rangle \rightarrow |D\rangle \rightarrow |B\rangle$. (c) Energy transfer between the bright and dark modes takes place by near-field coupling, with coupling constant κ. The Fano minimum is characterized by a combined phase shift from $|B\rangle \rightarrow |D\rangle$ and $|D\rangle \rightarrow |B\rangle$ equal to π, so that the two paths shown in (b) destructively interfere and cancel the polarization of the bright mode. (d) Calculated extinction spectrum and surface charge density plots for a nanoshell quadrumer, for normal incidence and the electric field oriented at 90°. The nanoshells have a geometry set to $[r_1/r_2]$ = [62.5/85] nm, where r_1 and r_2 are the core and shell radius, respectively, and their interparticle separation is 2.0 nm. The structure is embedded in a dielectric ellipse with a refractive index of 1.5. The Fano minimum, characterized by a pronounced spectral minimum, is at 1080 nm. The peaks of the interfering bright and dark modes are denoted by pink and black dashed lines, respectively.

processing, using electron beam lithography or focused ion beam milling.[8,12−14] An alternative to top-down fabrication is the bottom-up assembly of metal−dielectric colloids. Recently, it was demonstrated theoretically[9] and experimentally[11] that self-assembled clusters of seven metal−dielectric colloids support strong Fano-like resonances. With these clusters, the coupling between particles is strong and the Fano-like resonance can be tuned from the visible to the near-IR by varying structural parameters such as the particle geometry and interparticle separation.

In this Letter, asymmetric quadrumers of polymer-coated gold nanoshells are investigated as model systems for Fano-like interference. Individual clusters are assembled and analyzed with dark field scattering spectroscopy; details of the fabrication and experimental setup have been reported[11] and are discussed in the Supporting Information (see Figure S1). Nanoshells are spherical silica-core metal-shell nanoparticles with plasmonic resonances that are tunable based on their core−shell aspect ratio.[15,16] They are useful elements for cluster assembly because their synthesis and packing into clusters are highly controllable. Furthermore, clusters built from such isotropic colloidal units will generally support bright electric dipole modes for all incident electric field orientations, providing much flexibility in Fano-like resonance engineering. This work builds on the previous study[11] of seven-particle clusters, where the observed Fano-like resonance was isotropic in the plane of the structure. Here, only four particles are involved, which considerably simplifies the bottom-up assembly of the cluster. Furthermore, the analysis of this asymmetric quadrumer, together with the symmetric quadrumer, supports the detailed study of Fano-like resonances in the context of symmetry breaking.

To understand the origin of Fano-like interference in asymmetric clusters, it is useful to first examine the scattering spectra of a single nanoshell and of symmetric dimer and trimer clusters (Figure S2 in Supporting Information). These spectra each contain a bright electric dipole peak, but there are no Fano minima that strongly overlap with these modes. These structures do support many dark modes; however, they are either strongly blue shifted relative to the bright mode or do not couple to this mode due to symmetry considerations (discussed in detail later). To create dark modes that strongly overlap with and couple to the bright mode, additional mode engineering is required.

In one approach, spherical particles of different sizes or types can be packed into clusters; asymmetry can modify the dark modes and enable their strong interference with the bright mode.[4,7,17−20] Symmetry breaking has been previously utilized in colloidal systems involving solid gold−silver nanosphere dimers,[21] gold nanosphere−nanoshell dimers,[22] and nearly concentric gold nanosphere−nanoshell particles.[20] In another approach, additional identical nanoparticles can be added to create larger clusters. Here, new dark modes are created[9,23,24] that contribute to strong Fano-like resonances. This approach is the basis for the heptamer cluster,[9,11−13] which comprises seven identical particles packed in a hexagonal lattice. Strong Fano-like interference results from the interaction between the bright mode and a new type of dark mode, where the polarization of the outer ring of six particles is oriented oppositely to that of the inner particle. This approach is advantageous because identical nanoparticles are used, which simplifies cluster fabrication based on self-assembly. In the present study, we show that the asymmetric quadrumer is the simplest close-packed structure of identical spheres that supports strong Fano-like resonances.

We begin our analysis by examining the calculated extinction spectrum of the asymmetric quadrumer (Figure 1d). The bright mode is peaked at 900 nm, and its broad linewidth spans the entire wavelength range shown. The surface charge density plot for this mode at its peak intensity shows that the charge distribution on each nanoshell is predominantly dipolar and oriented in the same direction, resulting in strong scattering due to the constructive interference of their radiating fields. Fano-like interference is characterized by the narrow dip at 1080 nm. The corresponding

DOI: 10.1021/nl1029732 | *Nano Lett.* **2010,** *10,* 4680–4685

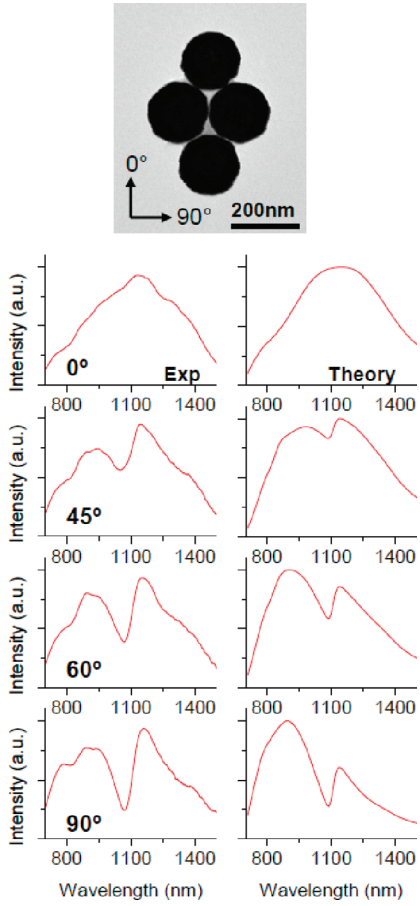

FIGURE 2. Scattering spectra of the quadrumer. TEM image and spectra of an asymmetric quadrumer. The orientation angles of the incident electric field relative to the cluster are shown in the TEM image. The experimental spectra show a Fano minimum at 1080 nm that varies with orientation angle and is strongest at 90°. The calculated spectra also show a Fano minimum with a similar resonant wavelength and dependence on orientation angle.

charge density plot at the Fano minimum shows only the dark mode, indicating resonant energy storage in this mode and suppression of the bright mode. The total dipole moment of the dark mode is small because the dipoles of the two nanoshells in the center are oriented oppositely to the top and bottom nanoshells. As a result, the scattered fields from the nanoparticles interfere destructively and the mode becomes subradiant.

The TEM image and scattering spectra for an asymmetric quadrumer are presented in Figure 2 for different orientations of the incident s-polarized electric field relative to the cluster. Unlike the extinction spectrum in Figure 1d, these scattering spectra do not include contributions from absorption. In addition, higher order modes, including the Fano-like dark mode, can couple directly with the incident light due to retardation effects created by the large incidence angle;[25] as a result, higher order mode peaks become visible throughout the spectra, and the Fano-like minimum becomes slightly less pronounced. At 0° orientation, the spectrum shows a smooth, broad electric dipole peak; at 45°, a narrow Fano minimum emerges at 1080 nm, which increases in magnitude for larger orientation angles. Calculated scattering spectra are also plotted in Figure 2 and show good agreement with the experimental spectra. As observed experimentally, these spectra display a clear Fano minimum at 1080 nm that is anisotropic with the orientation of the incident electric field.

These quadrumers are modeled with an interparticle separation of 2.0 nm and a nanoshell geometry of $[r_1, r_2] = [62.5, 85]$ nm, where $[r_1, r_2]$ correspond to the silica core and nanoshell radii, respectively. These nanoshell geometries are consistent with those from the experimental TEM image. It is difficult to definitively resolve interparticle separations on the order of 2 nm because TEM images are two-dimensional projections of three-dimensional structures; sample properties such as particle faceting and depth-of-field limitations in the TEM image can limit the resolution of this measurement.[26] A spacing of 2.0 nm is chosen by modeling clusters with various separations and choosing the calculated spectra that best matched those from the experiment. It is noted that, while these spacings are small, they are not in a regime that supports electron tunneling within the gaps, which typically occurs at distances smaller than 1 nm.[27,28] The simulated incidence angle, incident polarization, and numerical aperture of the collection objective match those of the experiment and are defined in the Supporting Information. The thin film substrate support is justifiably neglected in these calculations (see Figure S3 in Supporting Information). While a single set of spectra is shown here, the observed Fano minimum is a robust feature and is observed in nearly all individual asymmetric quadrumer structures. This was the case even when the quadrumer comprised a moderately polydisperse distribution of nanoshells (see Figure S4 in the Supporting Information).

The pronounced anisotropy of the Fano-like resonance in Figure 2 is caused by differences in the quadrumer geometry along its two symmetry axes. In particular, the interaction between the two central nanoshells of the cluster qualitatively changes as the polarization of the dark mode shifts from one axis to the other. To understand the underlying plasmonic interactions responsible for this anisotropy, we begin by analyzing the symmetric quadrumer, shown in Figure 3a. This structure supports an isotropic spectral response in the plane of the cluster due to its high degree of symmetry.[23] The two central nanoshells are separated by a large gap and couple very weakly with each other. The extinction spectrum of this structure reveals a broad, superradiant bright mode centered near 1000 nm. As with the bright modes in the asymmetric quadrumer, this mode consists of individual nanoparticle dipolar plasmons oscillating in the same orientation. A Fano-like resonance weakly overlapping with the bright mode is observed at 710 nm.

This cluster actually supports a host of dark modes, some of which strongly overlap in energy with the bright mode. An example is the magnetic mode,[23,29] which supports a

DOI: 10.1021/nl1029732 | *Nano Lett.* **2010,** *10,* 4680–4685

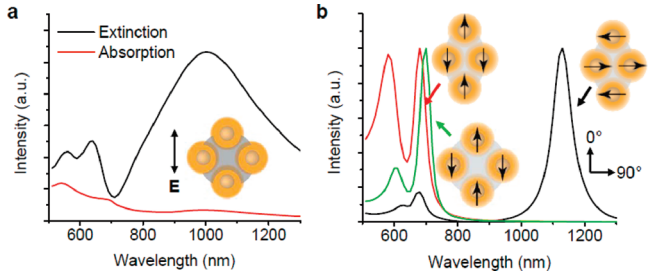

FIGURE 3. Symmetry breaking in quadrumers. (a) Calculated extinction and absorption spectra of a symmetric quadrumer. Dark modes capable of coupling with the bright electric dipole mode are all strongly blue shifted relative to the bright mode, and the structure therefore supports only a strongly blue shifted Fano-like resonance at 710 nm. (b) Calculated absorption spectra of dark modes for the symmetric and asymmetric quadrumer. The dark mode of the symmetric quadrumer and asymmetric quadrumer with 0° polarization orientation does not strongly overlap with the bright mode, while the dark mode of the asymmetric quadrumer with 90° polarization orientation strongly overlaps with the bright mode. This mode is strongly red shifted compared to the other dark modes due to longitudinal capacitive coupling between the two central nanoshells, which is characterized by an attractive Coulomb interaction between the surface charges of these nanoshells.

circulating displacement current and is slightly red shifted relative to the bright mode peak. The reason why many of these dark modes do not contribute to Fano-like resonances can be understood from group theory, which can be used to classify modes into different irreducible representations based on their symmetry. These representations form an orthogonal basis for the optical modes, and as such, only modes with the same irreducible representation can couple with each other. In prior analysis,[23] it was shown that optically active modes belong to the $2E_u$ irreducible representation. Therefore, only dark modes with $2E_u$ symmetry can couple with the bright cluster mode and contribute to Fano-like interference. The magnetic mode in the example above has A_{2g} symmetry and cannot couple with the bright mode; it consequently is not clearly observed in the scattering spectrum. An examination of all $2E_u$ modes of the symmetric quadrumer shows dark modes all strongly blue shifted relative to the bright electric dipole cluster mode,[23] resulting in Fano-like resonances that are strongly blue-shifted relative to the bright mode.

To clearly show the energies of the quadrumer dark modes in various cluster configurations, dark modes are directly simulated by exciting dipoles of the individual nanoshells with orientations shown in the insets of Figure 3b. In all cases, the dipole moments of the two central nanoshells oppose those of the top and bottom nanoshell, similar to that in Figure 1d. The dark mode spectrum of the symmetric quadrumer shows the mode near 710 nm that is responsible for the Fano minimum in Figure 3a. As the symmetric quadrumer deforms into an asymmetric quadrumer, the gap between the two central nanoshells reduces and the two particles strongly couple, leading to a highly polarization-dependent modification of the dark mode. The bright mode of the quadrumer also becomes orientation-dependent upon symmetry breaking; however, this dependence is not very strong: for all polarization orientations, this mode is characterized as a broad feature peaked between 800 and 1100 nm (Figure 2). This mode is somewhat insensitive to orientation because, for all polarization orientations, there is strong longitudinal capacitive coupling between nanoshells along the polarization direction. This coupling is characterized by a strong Coulomb attraction between the surface charges of the nanoshells, resulting in a strong mode red shift for all orientations. Additionally, the mode is strongly linewidth broadened for all orientations because the dipoles of the individual nanoshells are always aligned in the same direction, yielding superradiance.

For nanoshell polarizations oriented at 0°, the dark mode appears at 680 nm. As with the dark mode of the symmetric quadrumer, this mode contributes a Fano-like resonance that does not strongly overlap with the bright mode continuum. In this mode, the dipoles on the central nanoshells are parallel with one another, such that there exists Coulomb repulsion between the surface charges of the nanoshells. This causes the dark mode to blue shift slightly relative to that of the symmetric quadrumer, which does not support such coupling between the central nanoshells.

The spectrum of the asymmetric quadrumer with nanoshell polarizations oriented at 90° shows a strongly red shifted mode at 1100 nm. Here, the dark mode resonance is near the peak of the bright cluster mode (Figure 1d) and contributes to a strong Fano-like resonance (Figure 2). The substantial red shift observed for this particular symmetry breaking arises due to the strong longitudinal capacitive coupling between the two central nanoshells, similar to that supported by the bright mode described earlier. The fact that this dark mode is shifted to the red side of the bright mode (Figure 1d) indicates the presence of strong higher-order mode coupling (i.e., quadrupolar, octupolar, etc.) between nanoshells in this cluster. This additional coupling between neighboring nanoshells leads to further enhanced longitudinal capacitive coupling between nanoshells and further red shifts the mode; these contributions of multipolar coupling to red shifting can be quantified using plasmon hybridization.[30] These multipolar charge distributions on the nanoshells in the cluster can be inferred from the surface charge plot of the dark mode in Figure 1d, which displays highly nondipolar charge distributions on the nanoshells.

Nanostructures supporting strong Fano-like interference have a range of applications. One is nanoscale waveguiding, where the propagation of radiation along a chain of nanostructures at their Fano minimum can yield highly dispersive and relatively scatter-free waveguiding. These structures can also be used as optical cavities because they can store large amounts of energy in the dark mode. Their integration with gain media can lead to light amplification at this mode. An application for individual passive structures is localized surface plasmon resonance (LSPR) sensing, in which shifts in plasmon resonance energy are measured as a function

DOI: 10.1021/nl1029732 | *Nano Lett.* **2010,** *10,* 4680–4685

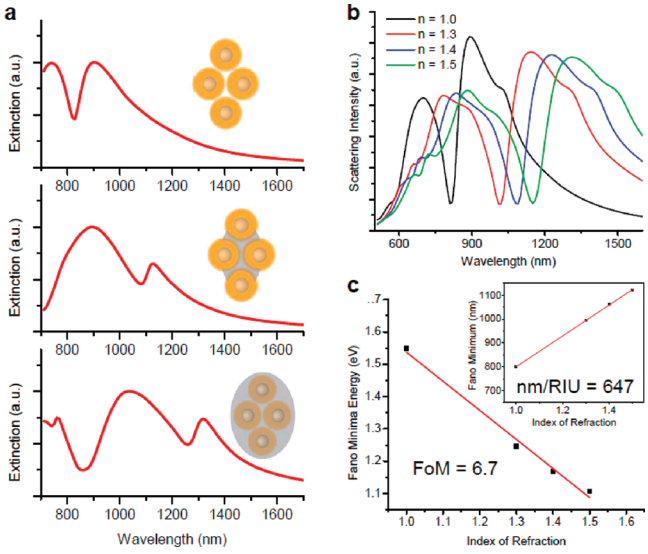

FIGURE 4. Calculated spectra of quadrumers in different dielectric environments. (a) The Fano minimum is highly sensitive to the surrounding dielectric environment and red shifts in the extinction spectra when embedded in either a small or large elliptical disk with dielectric constant $\varepsilon = 2.5$. The thin disk (middle) has dimensions $[R_1, R_2] = [179, 116]$ nm and is 30 nm thick, and the larger, thick disk (bottom) has dimensions $[R_1, R_2] = [284, 221]$ nm and is 250 nm thick. R_1 and R_2 are the major and minor axes, respectively, and the disks are aligned with the equatorial plane of the cluster. (b) Scattering spectra of a quadrumer embedded in environments of different index of refraction. (c) The calculated figure of merit, determined in part by the change in Fano minima energy as a function of local refractive index, is 6.7. The inset shows the calculated nm/RIU to be 647.

of the refractive index of the environment. Structures supporting Fano-like resonances are ideal for nanoscale LSPR sensing because they are particularly sensitive to the surrounding environment and have relatively narrow linewidths.[7,9,12,31,32] Calculated extinction and scattering spectra of the quadrumer in different dielectric environments are shown in Figure 4 and exhibit large sensitivity to the local environment. Figure 4a shows that even a thin dielectric disk insert can cause a significant red shift of the spectral position of the Fano minimum; this is consistent with the fact that most of the energy of the mode is localized at the gaps where the nanoshells are most closely spaced.[33]

The sensitivity of an LSPR sensor can be characterized by the figure of merit (FoM) defined as $(\Delta E/\Delta n)/(\text{linewidth})$,[34] where $\Delta E/\Delta n$ is the shift in surface plasmon resonance energy as a function of refractive index and the "linewidth" corresponds to the width of the plasmon resonance. For Fano-like resonances, the linewidth can be defined as the energy difference between the Fano minimum and the closest neighboring peak;[7] it is otherwise difficult to consistently define the linewidths of such highly asymmetric lineshapes. The ΔE and Δn parameters plotted in Figure 4c, taken from the scattering spectra in Figure 4b, yield a FoM of 6.7, which is similar to those experimentally and theoretically measured in related Fano structures.[9,12,31] This FoM is greater than those measured in individual gold and silver nanoparticles, which range from 0.9 to 5.4,[35] demonstrating the utility of Fano-like resonances in LSPR sensing. Another parameter that is used to characterize LSPR sensors is nm/RIU, which gauges the change of mode peak wavelength as a function of refractive index; as shown in the inset of Figure 4c, the nm/RIU of the quadrumer is 647. In practice, the polymer spacer in self-assembled quadrumers would need to be removed for the structure to support large FoMs and nm/RIUs. This may be achieved by various forms of chemical removal and may be expedited by judicious choice of the polymer; this will be the subject of future study.

In conclusion, we have demonstrated that the asymmetric quadrumer cluster supports a pronounced Fano minimum. The strength of this resonance strongly depends on the polarization of incident electric field, which is due to orientation-dependent capacitive coupling within the cluster. While this resonance was demonstrated using nanoshells, it is general to plasmonic systems of spherical particles such as solid spheres and hollow shells; the existence of the bright and dark modes as eigenmodes with the same irreducible representation originates from the symmetry of the quadrumer geometry itself. It is noted however that this analysis cannot be generalized to clusters comprising nonspherical particles such as cubes, as higher order mode coupling between such particles is different from spheres and is strongly orientation dependent. This structure has potential for a number of applications including LSPR sensing; its FoM and nm/RIU are calculated to be 6.7 and 647, respectively. This study demonstrates that simple, self-assembled nanostructures indeed have the capacity for interesting and unique optical modes and that they will play a large role in the swiftly growing field of coherent plasmonic engineering.

Acknowledgment. The work of J.F. and F.C. has been funded by the NSF NIRT under Grant No. 0709323. R.B., N.J.H., and P.N. acknowledge support from the DoD NSSEFF, the Robert A. Welch Foundation (C-1220 and C-1222), ARO, AFOSR, NSF under Grant No. CNS-0821727, and the Center for Advanced Solar Photophysics, and Energy Frontier Research Center funded by U.S. Department of Energy. G.S. and C.W. acknowledge funding by the Air Force Office of Scientific Research (AFOSR) Multidisciplinary University Research Initiative grants FA9550-06-1-0279 and FA9550-08-1-0394. J.B. acknowledges support from TcSUH and GEAR of the University of Houston, and the Robert A. Welch Foundation (E-1728). Electron microscopy was done at the Center for Nanoscale Science (CNS) at Harvard University. C.N.S. is a member of the National Nanotechnology Infrastructure Network. J.F. acknowledges Rodrigo Guerra for discussions and David Bell for electron microscopy support.

Supporting Information Available. Details of materals and methods, general analytic description of classical Fano-like interference, nanoshell cluster spectra, substrate effects, and robustness of the Fano minimum. This material is available free of charge via the Internet at http://pubs.acs.org.

DOI: 10.1021/nl1029732 | *Nano Lett.* **2010,** *10,* 4680–4685

REFERENCES AND NOTES

(1) Fano, U. *Phys. Rev.* **1961**, *124* (6), 1866–1878.
(2) Faist, J.; Capasso, F.; Sirtori, C.; West, K. W.; Pfeiffer, L. N. *Nature* **1997**, *390* (6660), 589–591.
(3) Alzar, C. L. G.; Martinez, M. A. G.; Nussenzveig, P. *Am. J. Phys.* **2002**, *70* (1), 37–41.
(4) Christ, A.; Ekinci, Y.; Solak, H. H.; Gippius, N. A.; Tikhodeev, S. G.; Martin, O. J. F. *Phys. Rev. B* **2007**, *76* (20), 201405(R).
(5) Zhang, S.; Genov, D. A.; Wang, Y.; Liu, M.; Zhang, X. *Phys. Rev. Lett.* **2008**, *101* (4), 047401.
(6) Papasimakis, N.; Fedotov, V. A.; Zheludev, N. I.; Prosvirnin, S. L. *Phys. Rev. Lett.* **2008**, *101* (25), 253903.
(7) Hao, F.; Sonnefraud, Y.; Van Dorpe, P.; Maier, S. A.; Halas, N. J.; Nordlander, P. *Nano Lett.* **2008**, *8* (11), 3983–3988.
(8) Verellen, N.; Sonnefraud, Y.; Sobhani, H.; Hao, F.; Moshchalkov, V. V.; Van Dorpe, P.; Nordlander, P.; Maier, S. A. *Nano Lett.* **2009**, *9* (4), 1663–1667.
(9) Mirin, N. A.; Bao, K.; Nordlander, P. *J. Phys. Chem. A* **2009**, *113* (16), 4028–4034.
(10) Liu, N.; Langguth, L.; Weiss, T.; Kastel, J.; Fleischhauer, M.; Pfau, T.; Giessen, H. *Nat. Mater.* **2009**, *8* (9), 758–762.
(11) Fan, J. A.; Wu, C. H.; Bao, K.; Bao, J. M.; Bardhan, R.; Halas, N. J.; Manoharan, V. N.; Nordlander, P.; Shvets, G.; Capasso, F. *Science* **2010**, *328* (5982), 1135–1138.
(12) Lassiter, J. B.; Sobhani, H.; Fan, J. A.; Kundu, J.; Capasso, F.; Nordlander, P.; Halas, N. J. *Nano Lett.* **2010**, *10* (8), 3184–3189.
(13) Hentschel, M.; Saliba, M.; Vogelgesang, R.; Giessen, H.; Alivisatos, A. P.; Liu, N. *Nano Lett.* **2010**, *10* (7), 2721–2726.
(14) Liu, N.; Langguth, L.; Weiss, T.; Kastel, J.; Fleischhauer, M.; Pfau, T.; Giessen, H. *Nat. Mater.* **2009**, *8* (9), 758–762.
(15) Oldenburg, S. J.; Averitt, R. D.; Westcott, S. L.; Halas, N. J. *Chem. Phys. Lett.* **1998**, *288* (2−4), 243–247.
(16) Pham, T.; Jackson, J. B.; Halas, N. J.; Lee, T. R. *Langmuir* **2002**, *18* (12), 4915–4920.
(17) Aydin, K.; Pryce, I. M.; Atwater, H. A. *Opt. Express* **2010**, *18* (13), 13407–13417.
(18) Davis, T. J.; Gómez, D. E.; Vernon, K. C. *Nano Lett.* **2010**, *10* (7), 2618–2625.
(19) Fedotov, V. A.; Rose, M.; Prosvirnin, S. L.; Papasimakis, N.; Zheludev, N. I. *Phys. Rev. Lett.* **2007**, *99* (14), 147401.
(20) Mukherjee, S.; Sobhani, H.; Lassiter, J. B.; Bardhan, R.; Nordlander, P.; Halas, N. J. *Nano Lett.* **2010**, *10* (7), 2694–2701.
(21) Bachelier, G.; Russier-Antoine, I.; Benichou, E.; Jonin, C.; Del Fatti, N.; Vallee, F.; Brevet, P. F. *Phys. Rev. Lett.* **2008**, *101* (19), 197401.
(22) Brown, L. V.; Sobhani, H.; Lassiter, J. B.; Nordlander, P.; Halas, N. J. *ACS Nano* **2010**, *4* (2), 819–832.
(23) Brandl, D. W.; Mirin, N. A.; Nordlander, P. *J. Phys. Chem. B* **2006**, *110* (25), 12302–12310.
(24) Zhang, W. H.; Gallinet, B.; Martin, O. J. F. *Phys. Rev. B* **2010**, *81* (23), 233407.
(25) Hao, F.; Larsson, E. M.; Ali, T. A.; Sutherland, D. S.; Nordlander, P. *Chem. Phys. Lett.* **2008**, *458* (4−6), 262–266.
(26) Marhaba, S.; Bachelier, G.; Bonnet, C.; Broyer, M.; Cottancin, E.; Grillet, N.; Lerme, J.; Vialle, J. L.; Pellarin, M. *J. Phys. Chem. C* **2009**, *113* (11), 4349–4356.
(27) Zuloaga, J.; Prodan, E.; Nordlander, P. *Nano Lett.* **2009**, *9* (2), 887–891.
(28) Perez-Gonzalez, O.; Zabala, N.; Borisov, A. G.; Halas, N. J.; Nordlander, P.; Aizpurua, J. *Nano Lett.* **2010**, *10* (8), 3090–3095.
(29) Alu, A.; Salandrino, A. *Opt. Express* **2006**, *14* (4), 1557–1567.
(30) Nordlander, P.; Oubre, C.; Prodan, E.; Li, K.; Stockman, M. I. *Nano Lett.* **2004**, *4* (5), 899–903.
(31) Liu, N.; Weiss, T.; Mesch, M.; Langguth, L.; Eigenthaler, U.; Hirscher, M.; Sonnichsen, C.; Giessen, H. *Nano Lett.* **2010**, *10* (4), 1103–1107.
(32) Sonnefraud, Y.; Verellen, N.; Sobhani, H.; Vandenbosch, G. A. E.; Moshchalkov, V. V.; Van Dorpe, P.; Nordlander, P.; Maier, S. A. *ACS Nano* **2010**, *4* (3), 1664–1670.
(33) Lassiter, J. B.; Aizpurua, J.; Hernandez, L. I.; Brandl, D. W.; Romero, I.; Lal, S.; Hafner, J. H.; Nordlander, P.; Halas, N. J. *Nano Lett.* **2008**, *8* (4), 1212–1218.
(34) Sherry, L. J.; Chang, S.-H.; Schatz, G. C.; Van Duyne, R. P.; Wiley, B. J.; Xia, Y. *Nano Lett.* **2005**, *5* (10), 2034–2038.
(35) Liao, H. W.; Nehl, C. L.; Hafner, J. H. *Nanomedicine* **2006**, *1* (2), 201–208.

DOI: 10.1021/nl1029732 | *Nano Lett.* **2010,** *10,* 4680–-4685